Title
A PULSE-HEIGHT COMPENSATION SYSTEM FOR Ge(Li) TIMING

Authors
Jaklevic, J.M.
Bernthal, F.M.
Radeloff, J.O.
et al.

Publication Date
1968-08-01

University of California

Ernest O. Lawrence Radiation Laboratory

A PULSE-HEIGHT COMPENSATION SYSTEM FOR Ge(Li) TIMING

J. M. Jaklevic, F. M. Bernthal, J. O. Radeloff,
and D. A. Landis

August 1968

Berkeley, California

DISCLAIMER

To be submitted to:
Nucl. Inst. Methods

UCRL-18389
Preprint

UNIVERSITY OF CALIFORNIA

Lawrence Radiation Laboratory
Berkeley, California

AEC Contract No. W-4705-eng-48

A PULSE-HEIGHT COMPENSATION SYSTEM FOR Ge(Li) TIMING

J. M. Jaklevic, F. M. Bernthal, J. O. Radeloff,
and D. A. Landis

August 1968

A PULSE-HEIGHT COMPENSATION SYSTEM FOR Ge(Li) TIMING*

J. M. Jaklevic, F. M. Bernthal, J. O. Radeloff
and D. A. Landis

August 1968

Abstract

A pulse-height compensation system for correcting the "energy walk" of Ge(Li) fast-timing data is described. The results of the method, applied to a number of different Ge(Li) detectors, are presented. A factor-of-two improvement in time resolution was found to be possible in all cases.

*This work was performed under the auspices of the U. S. Atomic Energy Commission.

1. Introduction

The importance of large volume Ge(Li) detectors in γ-ray coincidence measurements has prompted several investigations into the fast-timing characteristics of these devices.[1-3] One of the more significant results of these previous endeavors has been the realization that the charge collection time of the photopeak signal is not constant but depends in a complex manner upon the details of the interactions within the crystal producing a particular pulse. Since this variation is reflected in the rise-time of the pulses at the preamplifier output, it has become common practice to employ a leading edge discriminator to extract the timing information from the detector pulse. This method has the advantage over crossover or fractional amplitude pickoff timing of a smaller variation of trigger time with rise time variations but suffers the disadvantage of introducing a dependence of trigger time upon the energy of the pulse. Although this energy dependence is of little consequence in measurements involving coincidences between narrow energy regions of the Ge(Li) spectrum it can produce a significant broadening in the time resolution curve in the more frequently encountered cases in which one is interested in the full energy spectrum of γ-rays.

In the present paper we describe a Ge(Li) fast-timing system which employs a relatively simple method of compensating for the energy dependence of the timing signal. The results obtained using this system with several types of Ge(Li) detectors are shown. In addition, other measurements relevant to fast timing with Ge(Li) detectors are discussed.

2. Procedure

A block diagram of the electronics used in the present measurements is shown in Fig. 1. The bulk of the diagram is concerned with a conventional leading edge timing system. The pulse height compensation system is enclosed within the dashed lines.

The fast timing system makes use of the dual outputs provided by the high-rate linear amplifier in use at this laboratory.[4)] The output labeled SLOW has been subjected to optimum filtering for energy analysis. The FAST output is a parallel signal which bypasses the integrating stage of the amplifier and therefore retains the fast components of the Ge(Li) output. This method of obtaining the fast signal insures that the timing circuitry does not affect the energy resolution of the signal. It also provides an initial amplification stage before the wide band amplifier. In addition to being used for timing purposes, the signal from the FAST output is used as an input to the pile-up rejector. The pile-up rejector module enables one to reject both pile-up pulses and those with rise times greater than a certain threshold. The use of the module as shown in Fig. 1 is particularly effective in coincidence experiments where high counting rates are desired. Although the diagram shows a single (x10) wide band amplifier in the fast channels, it is sometimes possible to use two such units in cascade (if the signal/noise ratio is sufficiently large) to permit timing at a lower effective level on the signal.

In order to minimize the time variation as a function of rise time the discriminator is set as close as possible to the noise level of the amplifier output. The discriminator output is then used as one input to a "START-STOP" time-to-amplitude converter (TAC). In Fig. 1 both the "START" and "STOP" sides are identical although in some of the measurements discussed later a NaI scintillation detector system was substituted for the "START" side. The three-dimensional amplitude data were digitized and stored serially on incremental tape using an on-line PDP-7 computer multi-parameter data acquisition system.[5]) The system is normally used for γ-ray coincidence measurements and proved to be convenient for studying the energy dependence of the timing curves.

Operation of the pulse height compensation system can best be explained by considering Fig. 2. The upper curve is a plot of centroid position of the TAC output as a function of energy for a 13 mm depletion depth planar Ge(Li) detector. The source was Co^{60} and the "START" signal was provided by a NaI scintillation detector. The "error" bars are used to indicate the full width at half maximum (FWHM) of the time distribution. Analysis of the dependence of centroid position on energy shows that the time shift can be approximated by a function proportional to log E, where E is the energy of the signal. Therefore by mixing a signal proportional to log E with the time output one can essentially compensate for this energy dependence. This is accomplished by means of a logarithmic amplifier used in the configuration shown in Fig. 1. The lower curve in Fig. 2 is a plot of centroid positions taken under conditions identical to those for the upper curve, except that the compensation signal has been mixed with the TAC output. The compensated signal exhibits only a slight energy dependence over the range shown. This could be improved by a more careful adjustment of the logarithmic amplifier gain and perhaps by generating a more complex function than the simple logarithmic one used here.

A detailed description of the circuitry for the logarithmic element can be found in ref. 6. All of the components involved in the compensation network are contained in one module with front panel gain controls for each of the signals. The amplitude of the logarithmic signal relative to the TAC output can be varied, which makes it possible to optimize the compensation empirically.

The usual optimizing procedure consists of minimizing the FWHM of a time distribution of coincident 511-keV γ-rays from a Na^{22} source. Since the applied compensation has its greatest effect in the energy region below 500 keV, this procedure has proved to be both convenient and adequate.

3. Results

Four different Ge(Li) detectors were used in the following study of fast timing characteristics with and without pulse height compensation. The detectors and the parameters of interest were:

(1) 13 mm PLANAR - depletion depth = 13 mm, area = 8 cm^2, bias = 4750 V., resolution = 2.4 keV at 1173 keV, peak/compton = 14:1 (Co^{60} source).

(2) 10 mm PLANAR - depletion depth = 10 mm, area = 6 cm^2, bias = 2500 V., resolution = 2.1 keV at 1173 keV, peak/compton = 10:1 (Co^{60} source).

(3) "FIVE-SIDED" COAX - depletion depth = ~12 mm, volume ≅ 35 cm^3, bias = 1600 V., resolution = 3.2 keV at 1173 keV, peak/compton ≅ 20:1 (Co^{60} source).

(4) TRUE COAX - depletion depth = ~12 mm, volume ≅ 35 cm^3, bias = 2250 V., resolution = 2.6 keV at 1173 keV, peak/compton ≅ 20:1 (Co^{60} source).

Figure 3 is a plot of the Na^{22} time distribution obtained with the NaI detector and the 10 mm planar Ge(Li) detector. The plots represent uncompensated and compensated data respectively. As indicated in the figures, the broader distributions are data for all energies above threshold (~20 keV) while the narrower peaks include only events with energy greater than 100 keV. The broadening of the distribution in the former case is caused by the poor time resolution obtained at very low energies and by incomplete pulse height compensation due to the inadequacy of the Log E approximation at lower energies. In general, the effect of the low energy pulses on the time distribution is a very slight broadening at FWHM and a 10 - 20% broadening in the full width at tenth maximum (FW(0.1)M).

Figure 4 shows the data for the 13 mm planar and 10 mm planar detectors in coincidence. The two curves represent the uncompensated and compensated data for all energies above threshold.

As indicated previously two types of coaxial detectors were tested. Figure 5 is the time distribution obtained with a NaI detector and the true coaxial detector. The time resolution of this detector is considerably better than that of the "five-sided" detector. This result is consistent with previous observations[1,2] and is due to the non-uniform electric field in the end region of the detector. Figure 5 shows the data for the two coaxial detectors in coincidence.

Table 1 is a summary of the time-resolution measurement on the various detector configurations used. It is evident from the data that the pulse height compensation system effects a significant improvement in the time distribution. In general there is approximately a factor of 2 improvement in both FWHM and FW(0.1)M. Since the FW(0.1)M is a more realistic measure of the coincidence resolving time possible in a given configuration, one can conclude that using pulse height compensation resolving times of $2\tau = 29$ ns and $2\tau = 60$ ns are possible for planar-planar and coax-coax configurations respectively. Although this improvement is not as great as that which should be obtainable by using other techniques,[7,8,9] we feel that the simplicity of the method makes it attractive for a large number of applications.

The time resolution of a Ge(Li) diode is dependent upon the charge collection time of the holes and electrons in the device.[2] Since the drift velocity of the charge carriers in each diode is dependent upon the bias, a series of measurements was performed to determine the timing characteristics as a function of bias voltage for the two planar detectors used in this study. Figure 7 is a plot of the FWHM and FW(0.1)M obtained for the two detectors as the bias is increased. The 10 mm detector exhibits what might be termed "normal" behavior since the time resolution improves rapidly up to ~100 V/mm at which point the saturation velocity for holes and electrons is thought to be reached.[10]

Beyond that point there is only a very slight improvement in timing characteristics as the bias is increased. The curves for the 13 mm detector exhibit similar trends but do not level off until a bias of ~190 V/mm is reached. Observations of photopeak energy resolution vs bias voltage for this particular detector show that below ~190 V/mm this detector exhibits considerable tailing in the photopeak distribution. This effect is thought to be due to imperfections in the germanium which cause electric field irregularities in the drifted region below a certain critical field strength. This explanation would also account for the anomalous timing characteristics observed.

4. Acknowledgments

The authors wish to express their appreciation to Drs. C. M. Lederer, F. S. Goulding, and J. M. Hollander for their continuing interest and helpful comments. We especially thank Dr. Richard Pehl and the Berkeley detector group for their cooperation in supplying us with the Ge(Li) detector systems.

Table 1

Detector 1	Detector 2	Energy Range[a]	Energy Range[a]	FWHM (ns) Uncompensated	FWHM (ns) Compensated	FW(0.1)M (ns) Uncompensated	FW(0.1)M (ns) Compensated
13 mm Planar	NaI	Above Threshold	511 keV Photopeak	14.8	6.6	37.3	15.9
		Above 100 keV	511 keV Photopeak	14.6	6.4	27.9	13.9
		511 keV Photopeak	511 keV Photopeak		5.0		9.7
10 mm Planar	NaI	Above Threshold	511 keV Photopeak	12.3	5.6	29.4	12.5
		Above 100 keV	511 keV Photopeak	12.0	5.3	21.5	10.9
		511 keV Photopeak	511 keV Photopeak		4.1		7.7
13 mm Planar	10 mm Planar	Above Threshold	Above Threshold	20.0	9.1	59.5	23.8
		Above 50 keV	Above 50 keV	18.9	9.0	49.0	21.0
		511 keV Photopeak	511 keV Photopeak	6.3	6.4	12.0	12.0
"True" Coax	NaI	Above Threshold	511 keV Photopeak	17.0	10.7	40.6	23.1
		Above 100 keV	511 keV Photopeak	16.4	10.2	31.3	21.4
		511 kev Photopeak	511 keV Photopeak		7.7		15.0

Table 1 (Continued)

Detector 1	Detector 2	Energy Range[a]	Energy Range[a]	FWHM (ns)		FW(0.1)M (ns)	
				Uncompensated	Compensated	Uncompensated	Compensated
"5-Sided" Coax	NaI	Above Threshold	511 keV Photopeak	28.6	17.9	72.0	49.4
"True" Coax	"5-Sided" Coax	Above 50 keV	Above Threshold	33.7	20.1	91.2	57.6

[a]The Energy Range described as "Above Threshold" refers to the low energy cutoff for the entire system including PILE-UP REJECTOR and ADC Thresholds. This limit was approximately 20 keV for the cases cited above.

References

1) R. L. Graham, I. K. McKenzie and G. T. Ewan, IEEE Trans. Nucl. Sci. 13, no. 1 (1966) 72.

2) G. T. Ewan, R. L. Graham and I. K. McKenzie, IEEE Trans. Nucl. Sci. 13, no. 3 (1966) 297.

3) J. Pigneret, J. J. Samueli and H. Sarazin, IEEE Trans. Nucl. Sci. 13, no. 3 (1966) 306.

4) F. S. Goulding, D. A. Landis and R. H. Pehl, University of California, Lawrence Radiation Laboratory Report UCRL-17560 (1967).

5) L. B. Robinson and J. D. Meng, "Multiparameter Data System," Privately circulated report, (June 1967).

6) F. S. Goulding, D. A. Landis, J. Cerny and R. H. Pehl, Nucl. Instr. and Meth. 31 (1964) 1.

7) J. P. Fouan and J. P. Passerieux, Nucl. Instr. and Meth. 62 (1968) 327.

8) S. Gorni, G. Hochner, E. Nadav, and H. Zmora, Nucl. Instr. and Meth. 53 (1967) 349.

9) B. T. A. McKee, Nucl. Instr. and Meth. 62 (1968) 333.

10) F. S. Goulding, Nucl. Instr. and Meth. 43 (1966) 1.

Figure Captions

Fig. 1. Block diagram of fast-timing electronics. The pulse height compensation system is enclosed by dashed lines.

Fig. 2. Plot of centroid position as a function of energy for a 13 mm depletion depth planar Ge(Li) detector. The "error" bars are used to indicate the full width at half maximum (FWHM) of the time distribution. The upper curve is without compensation; the lower curve shows the effect of mixing the log E compensation signal with the TAC output.

Fig. 3. Timing curves obtained with a 10 mm depletion depth planar Ge(Li) detector in coincidence with a NaI scintillation spectrometer showing the effect of pulse height compensation on the time distribution. Curves are shown for both the full energy spectrum (all events above approximately 20 keV) and the spectrum of events with energies greater than 100 keV. The "STOP" signal was supplied by the Ge(Li) detector.

Fig. 4. Uncompensated and compensated timing curves for a 13 mm planar Ge(Li) detector in coincidence with a 10 mm planar Ge(Li) detector. All events corresponding to energies greater than approximately 20 keV are included. The "START" signal was supplied by the 13 mm detector, the "STOP" signal by the 10 mm detector.

Fig. 5. Uncompensated and compensated timing curves for NaI scintillation spectrometer in coincidence with the "5 sided" coaxial detector. All events corresponding to energies greater than approximately 20 keV are included. The "STOP" signal was supplied by the Ge(Li) detector.

Fig. 6. Uncompensated and compensated curves for "5 sided" coaxial detector in coincidence with the "true" coaxial detector. All events corresponding to energies greater than approximately 20 keV are included. The "START"

signal was supplied by the "5 sided" coaxial detector; the "STOP" signal by the "true" coaxial detector.

Fig. 7. Plot of full width at half maximum (FWHM) and full width tenth maximum (FW(0.1)M) as a function of applied bias field for the two planar detectors used in the measurements.

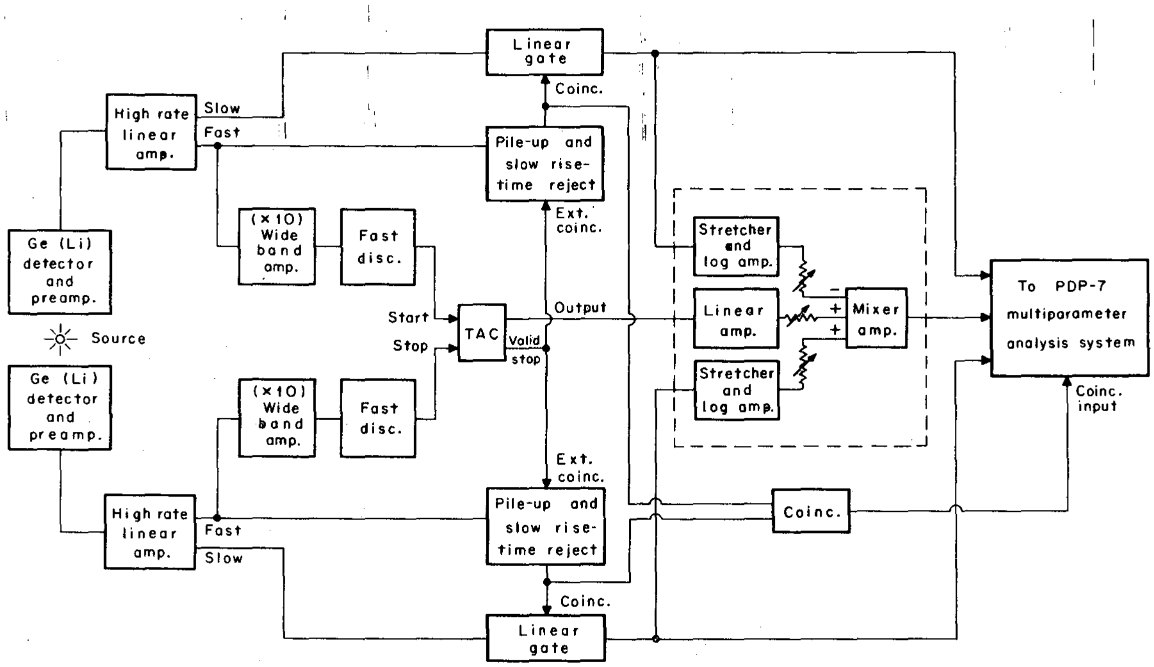

XBL688-3585

Fig. 1

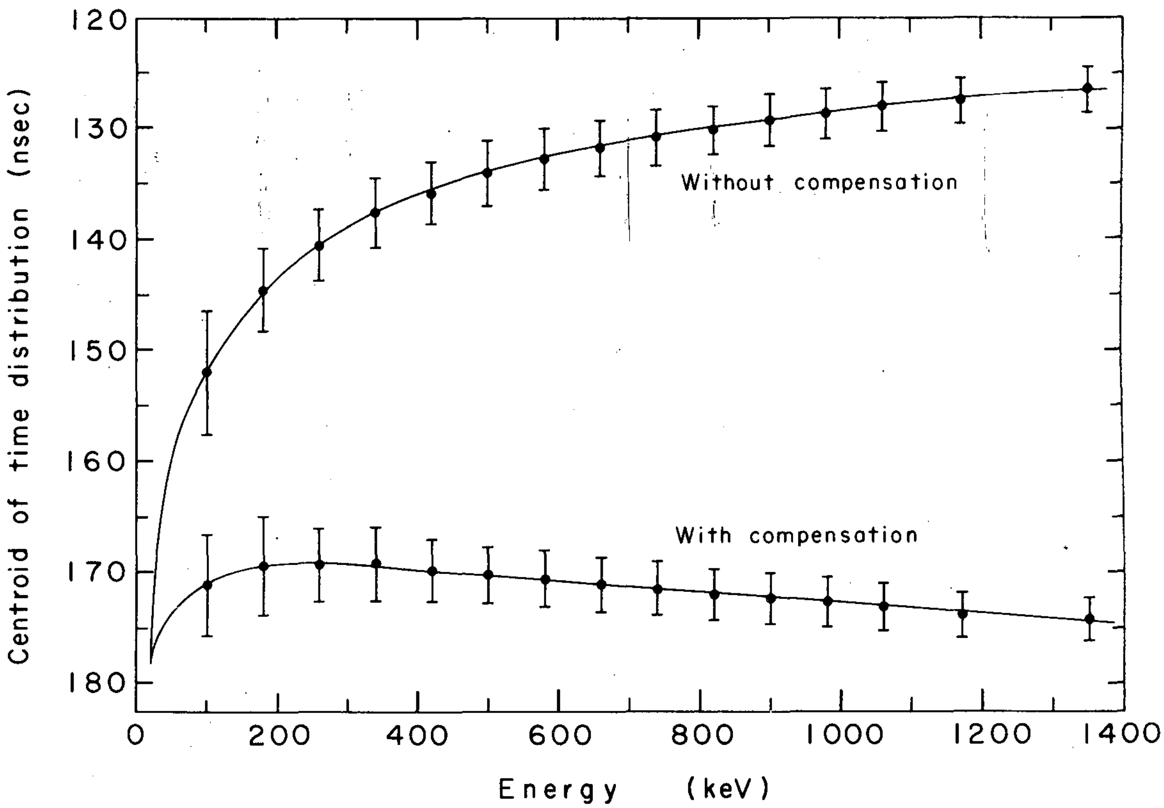

XBL688-3586

Fig. 2

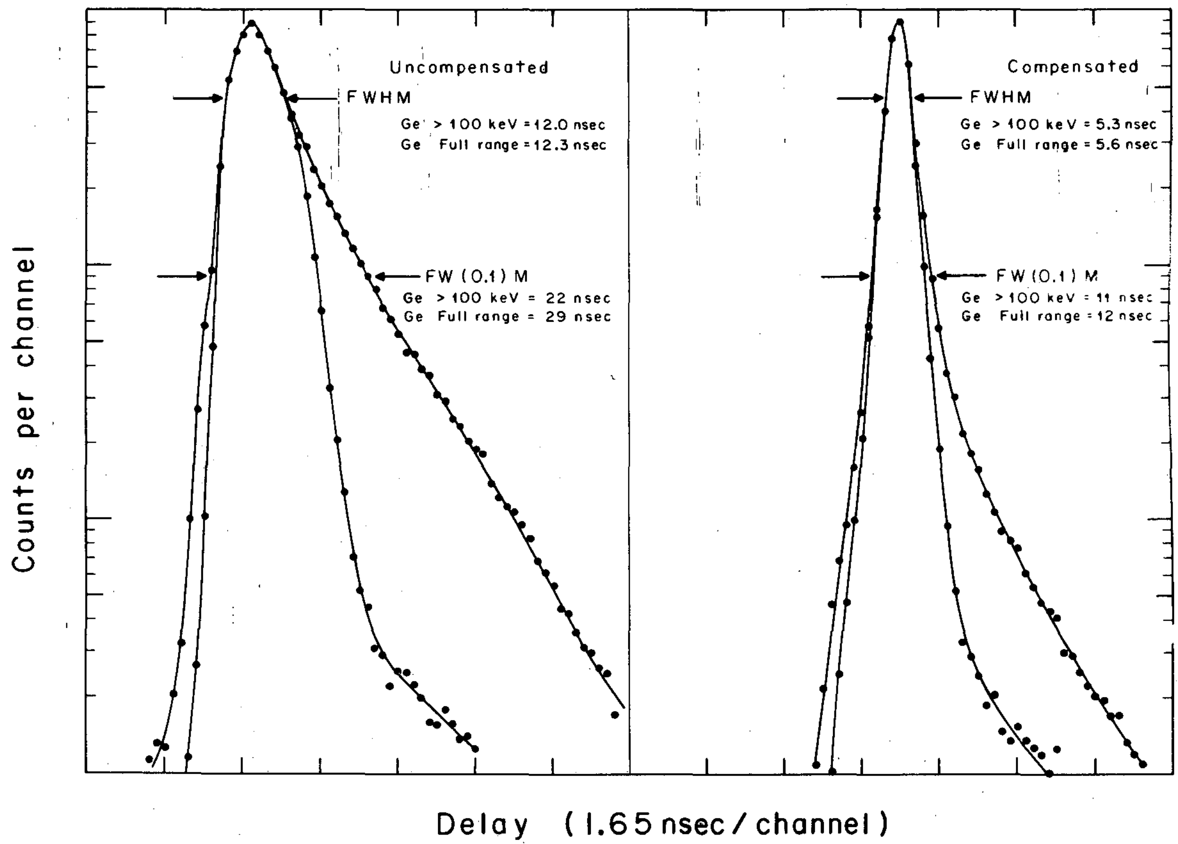

XBL688-3587

Fig. 3

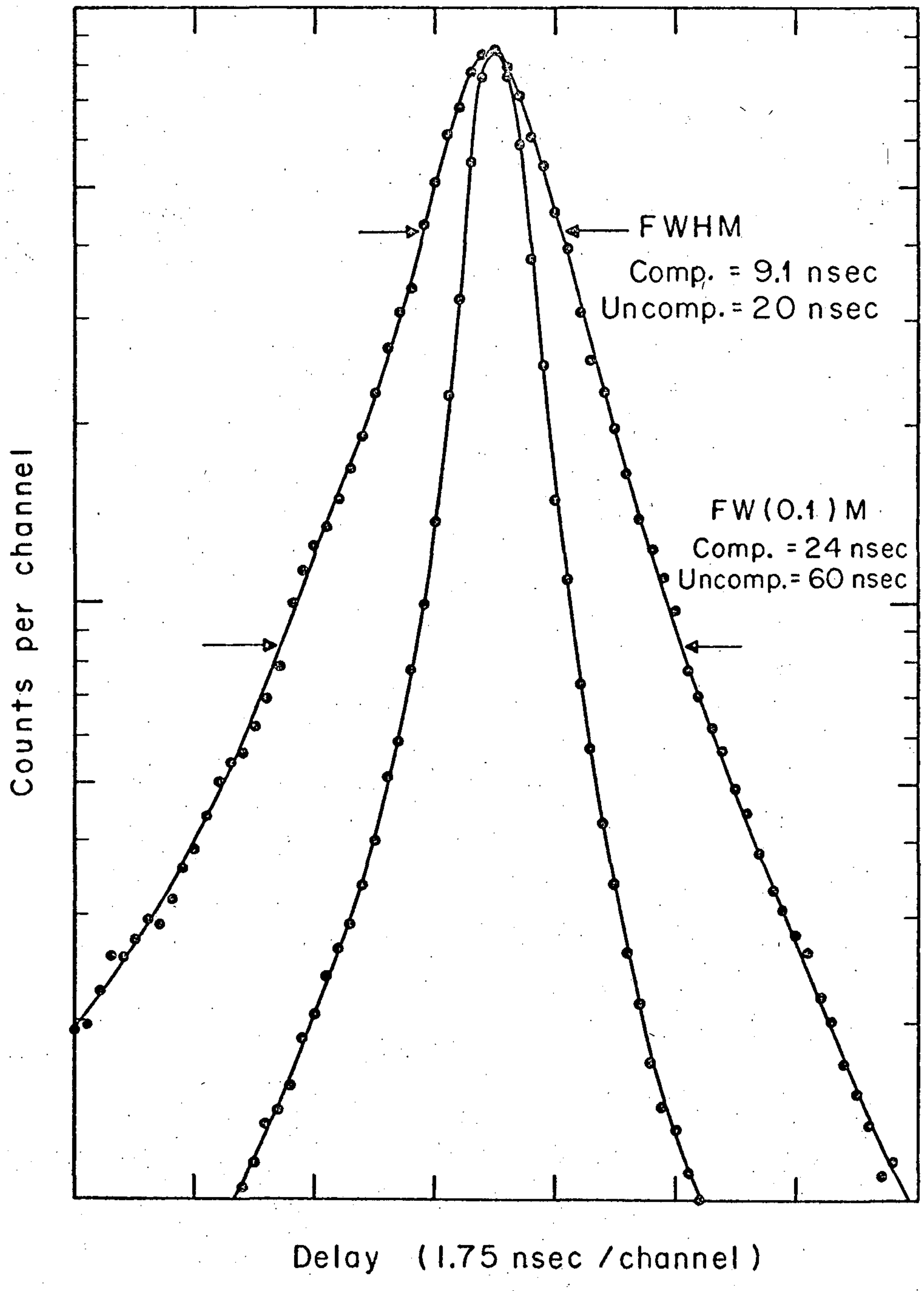

XBL688-3588

Fig. 4

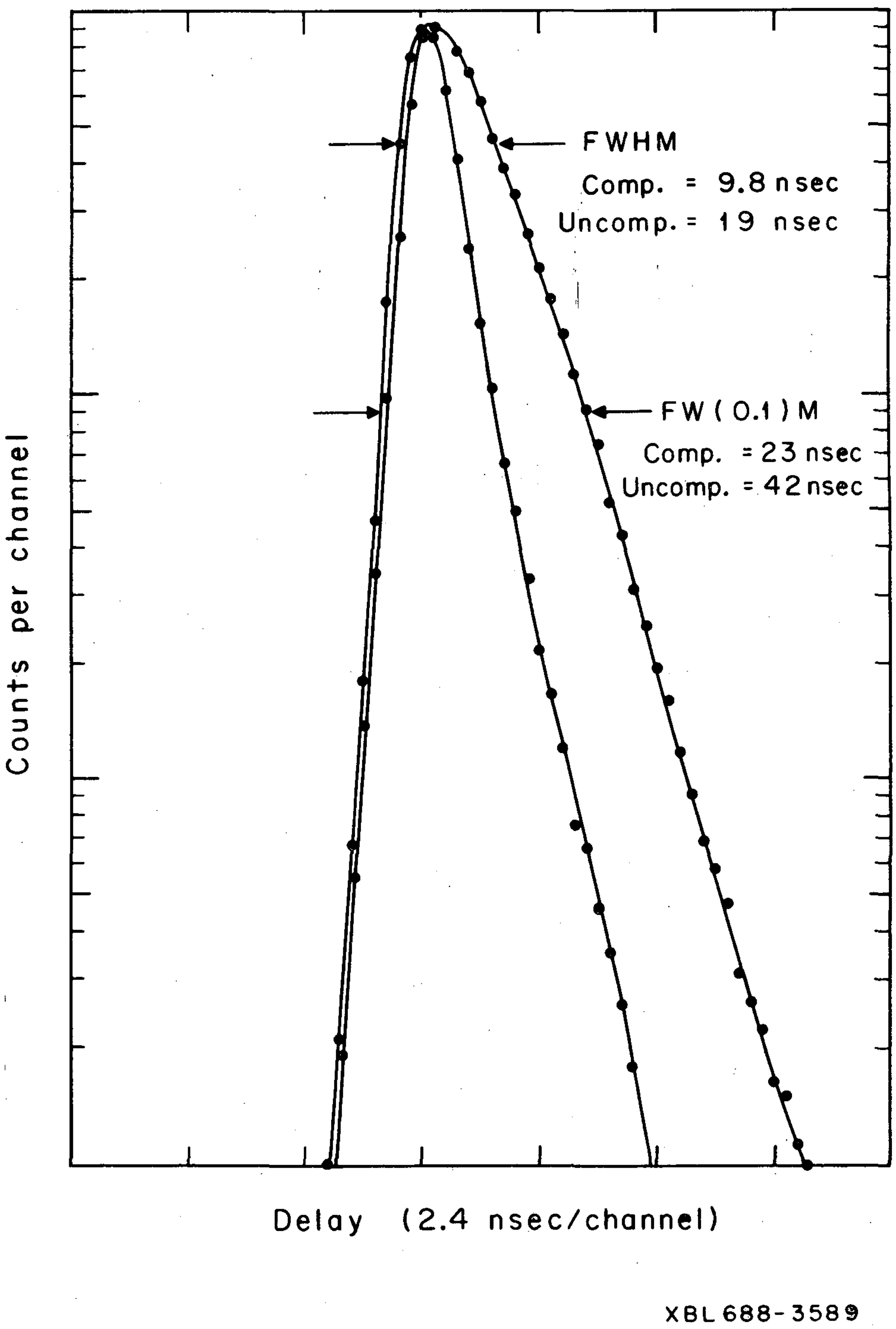
FWHM
Comp. = 9.8 nsec
Uncomp. = 19 nsec
FW(0.1)M
Comp. = 23 nsec
Uncomp. = 42 nsec
Counts per channel
Delay (2.4 nsec/channel)
XBL 688-3589

Fig. 5

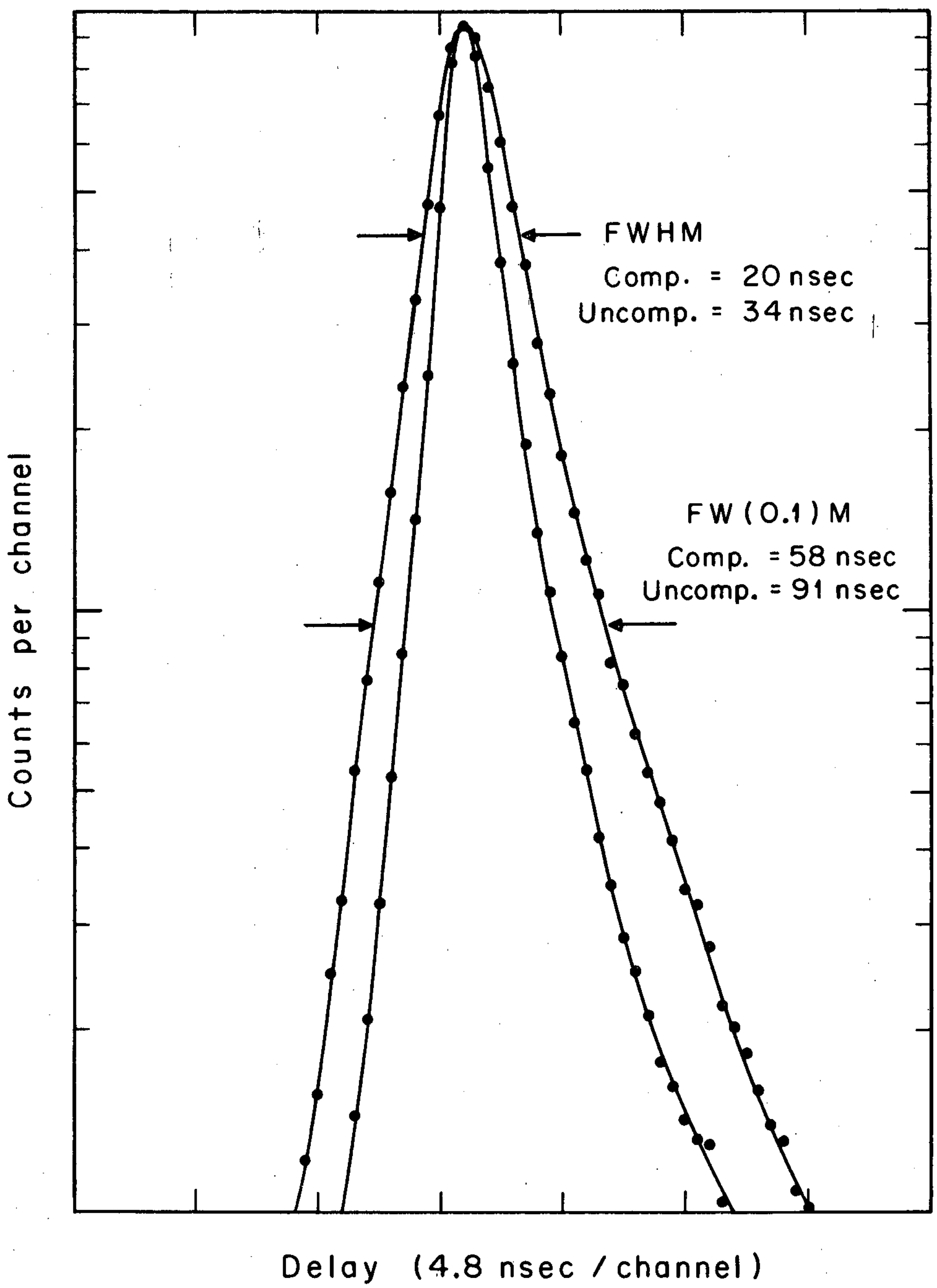

XBL688-3590

Fig. 6

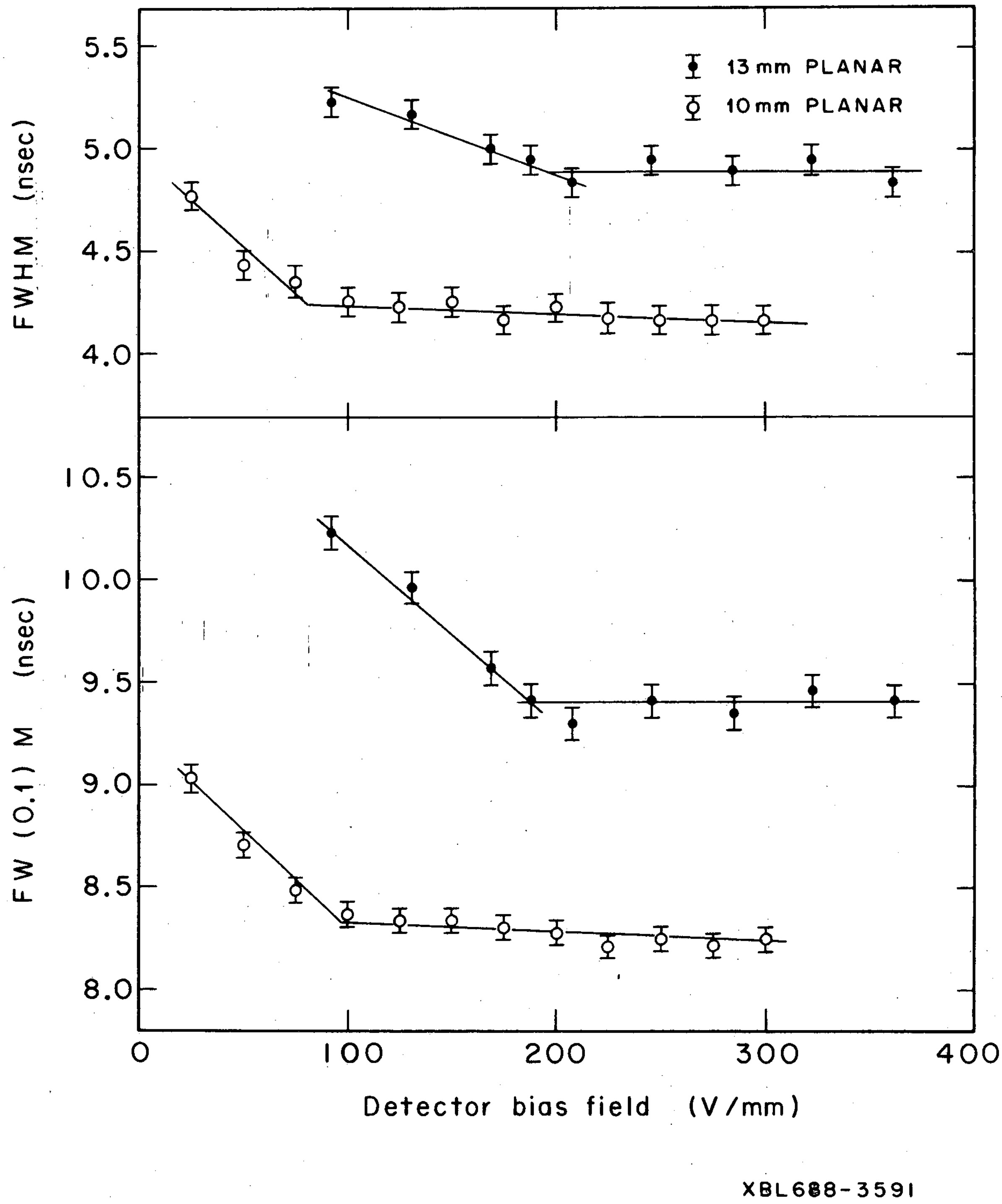
5.5
5.0
4.5
4.0
FWHM (nsec)
13 mm PLANAR
10 mm PLANAR
10.5
10.0
9.5
9.0
8.5
8.0
FW (0.1) M (nsec)
0
100
200
300
400
Detector bias field (V/mm)
XBL688-3591

Fig. 7